Analysis of the Underlying Mechanism of Frank-Starling Law of a Constructive Hemodynamics Model

Mitsuharu Mishima[1] , Takao Shimayoshi[2] , Akira Amano[3] , Tetsuya Matsuda[1]

[1]Graduate School of Informatics, Kyoto University, Japan
[2]ASTEM Research Institute of Kyoto, Japan
[3]Department of Bioinformatics, Ritsumeikan University, Japan

Abstract— Frank-Starling law, which describes a relation between cardiac contraction energy and end-diastolic volume, is of importance, but the detailed mechanism is not quantitatively understood yet. In this paper, the mechanism of a linear relation between end-diastolic volume and end-systolic pressure as a part of Frank-Starling law is analyzed by means of computer simulation. A hemodynamics model, which is constructed by composing a vascular system model, a left ventricular dynamics model and a myocardial cell model, reproduced a linear relation between end-diastolic volume and end-systolic pressure successfully. In this paper, the simulation results and the detailed analysis are reported.

Keywords— myocardial cell model, excitation-contraction coupling model, hemodynamic simulation, Frank-Starling law, circulatory equilibrium

1 Introduction

It is important to understand the detailed mechanisms of the heart, which is an organ to circulate blood into the whole body. A well known law on a cardiac function, Frank-Starling law[1] describes that the energy of myocardial contraction is proportional to the end-diastolic volume within the physiological range. The mechanism is qualitatively explained as the following[2]; 1) as the blood inflow to the heart increases, end-diastolic volume increases and ventricular wall is strongly stretched, 2) the resting myocardial length is stretched, thus myocardial tension increases according to length-tension relation, 3) as a result stroke volume increases, and the cardiac stroke work increases finally.

Another important relationship on the cardiac function is end-systolic pressure volume relation (ESPVR), which is expressed by the line connecting the point at end-systole of pressure-volume diagram and the points of other loads. ESPVR of a human heart is linear in physiological conditions, and the slope is called $\mathrm{E_{max}}$[3], which is an important clinical index of cardiac function. Pressure-volume area (PVA) is the area surrounded by a pressure-volume loop of a cardiac cycle and ESPVR. PVA indicates the total energy of external mechanical work and mechanical potential energy[4].

Although Frank-Starling law is an important empirical law to represent the relation between the load of heart and cardiac output, the underlying mechanism is not well understood yet. ESPVR and PVA show relationship between end-systolic pressure and cardiac energy consumption. Experimental results show a linear relation between end-diastolic volume and end-systolic pressure. This linear relation is an important factor of Frank-Starling law. Therefore, a detailed analysis of the linear relation between end-diastolic volume and end-systolic pressure helps understanding the mechanism of Frank-Starling law.

Computer simulation is an important technique to analyze and understand the mechanism of biological functions. In this study, the linear relation between end-diastolic volume and end-systolic pressure is analyzed by a circulation dynamics simulation. The model employed in the simulation is not made with a system identification approach, but composed of physiologically validated models. In this paper, the simulation results and the analysis are reported.

2 Model and Simulation Result

2.1 Hemodynamic model

In this study, a human infantile hemodynamics model proposed by Nobuaki et al.[5] (Nobuaki model) was used with some modifications. Nobuaki model, which can simulate baroreceptor reflex against modulations of the head-up tilt angle of the body, is composed of a vascular system model, a left ventricular dynamic model and a myocardial cell model. The vascular system model represents the dynamic change of systemic blood pressure, blood flow and left ventricular volume. The left ventricular dynamics model defines the relationship between the left ventricular volume and pressure, where the volume is related to the length of a myocardial cell and the pressure to tension by a myocardial cell. The myocardial cell model expresses and the developed tension of a myocardial cell.

The vascular system model in Nobuaki model is based on an adult vascular system model by Heldt et al.[6] The vascular system is expressed as an electric circuit, where a blood pressure is represented as a voltage and a blood flow as a current. The circuit consists of twelve compartments such as the heart, the aorta, the peripheral circulation, the vein and the pulmonary circulation. The each compartment is composed of a resistance, a linear capacitance, and a non-linear and time-variable capacitance. The left ventricular volume is expressed as the difference between the total blood volume and the blood volume of all compartments other than the left

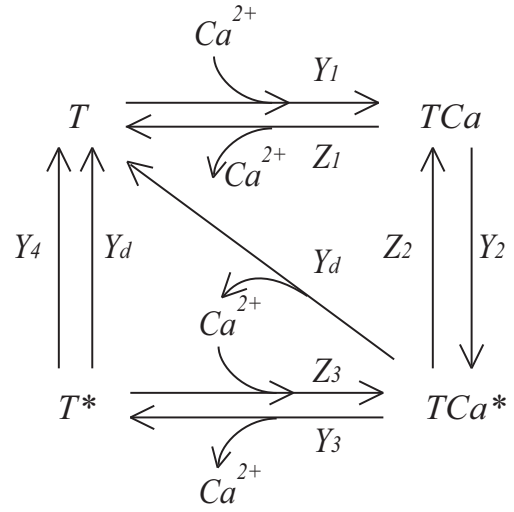

Figure 1: Four chemical states of Negroni-Lascano model

ventricle. Modulation of the body tilt angle varies the load of the heart through change of the blood distribution. In the current study, the adrenergic effect of baroreceptor reflex is removed from original Nobuaki model.

In the left ventricular system model, the relationship between the left ventricular pressure and the tension of the myocardial cell is expressed with Laplace formula:

$$\frac{P}{h} = \frac{F}{R}, \tag{1}$$

where P is the left ventricular pressure, h is the left ventricular wall thickness, F is the myocardial cell tension and R is the left ventricular radius. The relation between the left ventricular volume and the half sarcomere length of a myocardial cell is modified from the original formulation in order to fit experimental data and is formulated as

$$L = c_1 \cdot V + c_2, \tag{2}$$

where L is the half sarcomere length, V is the left ventricular volume, and c_1 and c_2 are constants.

Kyoto model[7] which is a comprehensive physiological model of a myocardial cell is used as myocardial cell model. Kyoto model precisely expresses membrane excitation and excitation-contraction coupling as ordinary differential equations by modeling each cellular component function such as ion channels, calcium buffering and myofibril. Kyoto model incorporates with a cardiac muscle model reported by Negroni and Lascano (Negroni-Lascano model) [8] with some modifications for excitation-contraction coupling.

2.2 Excitation-contraction coupling model

The excitation-contraction coupling model of Kyoto model describes cellular contraction mechanism as a four chemical states of troponin C as shown in Fig. 1; free troponin C (T), calcium ion bound troponin C (TCa), calcium ion bound troponin C with attached cross-bridges ($TCa*$), and troponin C without calcium ion but with attached cross-bridges ($T*$). The net rates of state transitions are expressed as following.

$$T \rightarrow TCa:$$
$$Q_1 = Y_1 \cdot [Ca^{2+}] \cdot p(T) - Z_1 \cdot p(TCa), \tag{3}$$
$$TCa \rightarrow TCa*:$$
$$Q_2 = Y_2 \cdot f_{OL}(L) \cdot p(TCa) - Z_2 \cdot p(TCa*), \tag{4}$$
$$TCa* \rightarrow T*:$$
$$Q_3 = Y_3 \cdot p(TCa*) - Z_3 \cdot [Ca^{2+}] \cdot p(T*), \tag{5}$$
$$T* \rightarrow T:$$
$$Q_4 = Y_4 \cdot p(T*) + Y_d \cdot f_{CB}(dX/dt) \cdot p(T*), \tag{6}$$
$$TCa* \rightarrow T:$$
$$Q_5 = Y_d \cdot f_{CB}(dX/dt) \cdot p(TCa*), \tag{7}$$

where Y_1-Y_4, Y_d, Z_1-Z_3 are rate parameters as defined below. $f_{OL}(L)$ is an overlap function to represent probability of state of TCa which can be used to form cross-bridges and defined as

$$f_{OL}(L) = \exp\left\{-20\,(L - 1.17)^2\right\}. \tag{8}$$

$f_{CB}(dX/dt)$ is defined as

$$f_{CB}(dX/dt) = \begin{cases} (dX/dt)^2/50 & (dX/dt > 0) \\ (dX/dt)^2 & (dX/dt \leq 0) \end{cases}, \tag{9}$$

$$\frac{d}{dt}X = B \cdot ((L - X) - h_c), \tag{10}$$

where B is a proportional constant and h_c the equivalent cross-bridges elongation, and $L - X$ represents cross-bridge elongation and dX/dt the velocity of motion of the mobile cross-bridge end. The rate constants depend on ATP concentration factors as the following:

$$Y_1 = 31.2 \quad [\mathrm{mM/msec}] \tag{11}$$
$$Z_1 = 0.06 \quad [\mathrm{msec}^{-1}] \tag{12}$$
$$Y_2 = 0.0039 \cdot \left(0.54 \cdot \frac{K_d PI_i}{K_d PI_i + [PI]} + 0.64\right) \quad [\mathrm{msec}^{-1}] \tag{13}$$
$$Z_2 = 0.0039 \cdot \frac{1}{1 + \left(\frac{K_d ATP_i}{[ATP_{total}]}\right)^3} \quad [\mathrm{msec}^{-1}] \tag{14}$$
$$Y_3 = 0.06 \quad [\mathrm{msec}^{-1}] \tag{15}$$
$$Z_3 = 1248 \quad [\mathrm{mM/msec}] \tag{16}$$
$$Y_4 = 0.12 \cdot \frac{1}{1 + \left(\frac{K_d ATP_i}{[ATP_{total}]}\right)^3} \quad [\mathrm{mM/msec}] \tag{17}$$
$$Y_d = 8000 \cdot \frac{1}{1 + \left(\frac{K_d ATP_i}{[ATP_{total}]}\right)^3} \quad [\mathrm{msec}/\mu\mathrm{m}^2], \tag{18}$$

where $K_d PI_i$ is a dissociation constant for PI and $K_d ATP_i$ is a dissociation constant for ATP. The derivatives of state

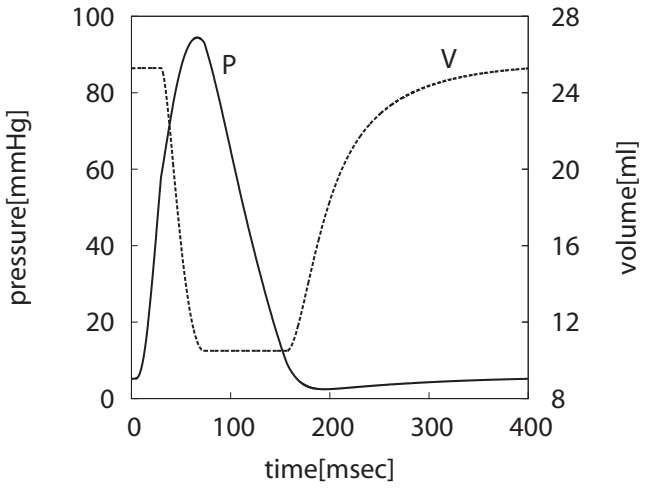

Figure 2: The time courses of pressure and volume at $\alpha = 0°$

probabilities are expressed as

$$\frac{d}{dt}p(T) = -Q_1 + Q_4 + Q_5 \tag{19}$$

$$\frac{d}{dt}p(TCa) = Q_1 - Q_2 \tag{20}$$

$$\frac{d}{dt}p(TCa*) = Q_2 - Q_3 - Q_5 \tag{21}$$

$$\frac{d}{dt}p(T*) = Q_3 - Q_4. \tag{22}$$

The developed tension of elongation element (F_b) is expressed as a product of cross-bridges concentration and cross-bridge elongation:

$$F_b = A \cdot [T_t] \cdot (p(TCa*) + p(T*)) \cdot (L - X), \tag{23}$$

where A is a constant and $[T_t]$ is total troponin concentration. The force developed by the parallel elastic element (F_p) is expressed as

$$F_p = \begin{cases} K_l(0.97 - L) & (L < 0.97) \\ K_l(0.97 - L) - K_p(L - 0.97)^5 & (L \geq 0.97) \end{cases}, \tag{24}$$

where $K_l (= 20[\mathrm{mN/mm^2}/\mu\mathrm{m}])$ and $K_p (= 140,000$ $[\mathrm{mN/mm^2}/\mu\mathrm{m}^5])$ are the intracellular passive stiffness. Finally, the tension of myocardial cell (F_{ext}) is expressed with F_b and F_p as

$$F = F_b - F_p. \tag{25}$$

2.3 Simulation result

Simulations were conducted under multiple body tilt angles (α) from $0°$ to $90°$ at every $15°$. The change of tilt angle alters the systemic blood pressure and cardiac workload. To convergent to the steady state, 40 cardiac cycles were simulated and the final cardiac cycles were analyzed. The simulations were performed with a simulation software "simBio"[9].

Fig. 2 shows the time course of pressure and volume at $\alpha = 0°$. Fig. 3 shows pressure-volume curve under different values of α. ESPVR is illustrated with a solid line as the relation between pressure and volume at end-systolic time (t_{es}). The obtained ESPVR is linear with the coefficient of determination $R^2 = 0.999$. Fig. 4 shows a relationship between end-diastolic volume $V(t_{ed})$ and end-systolic pressure $P(t_{es})$. The dots in Fig. 4 represent the result of each α, and the straight line is the regression line. The relation between $V(t_{ed})$ and $P(t_{es})$ is linear with $R^2 = 0.999$.

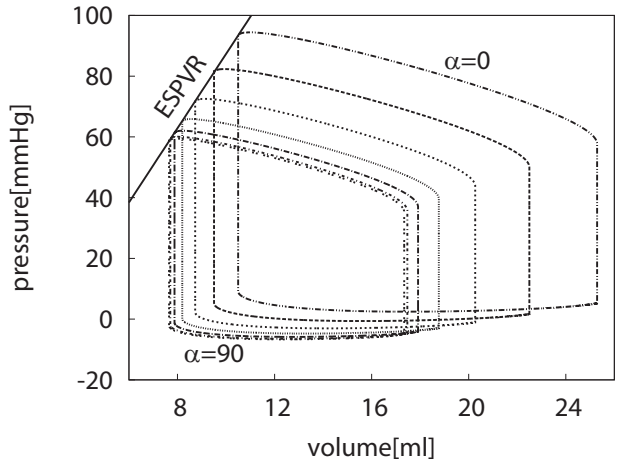

Figure 3: The pressure-volume curve and ESPVR

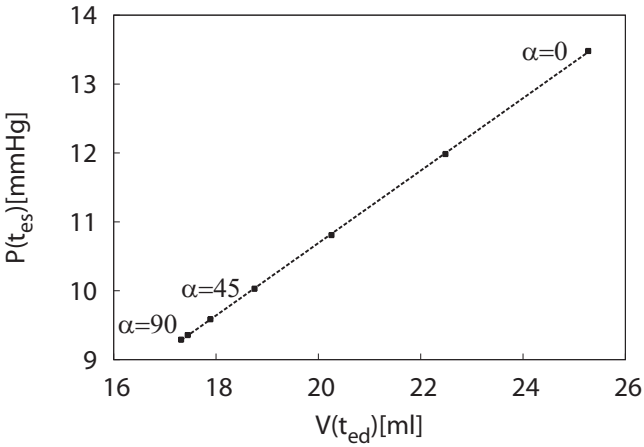

Figure 4: The relationship between $V(t_{ed})$ and $P(t_{es})$

3 Analysis

The details of the simulation results were analyzed to explain the linear relation between end-systolic pressure and end-diastolic volume. The left ventricular volume has a linear relation with the half sarcomere length of the myocardial cell as defined in Eq. 2. Although the left ventricular pressure depends not only on the tension of the myocardial cell but also on the wall thickness and the radius as defined in Eq. 1, the wall thickness and the radius have a weak dependency on the myocardial cell tension. Consequently, the relation between the half sarcomere length at end-diastole and the tension of the myocardial cell at end-systole is approximately linear ($R^2 = 1.000$) as shown in Fig. 5.

As defined in Eq. 25, the tension of the myocardial cell is a difference of F_b and F_p. Because the non-linear term of

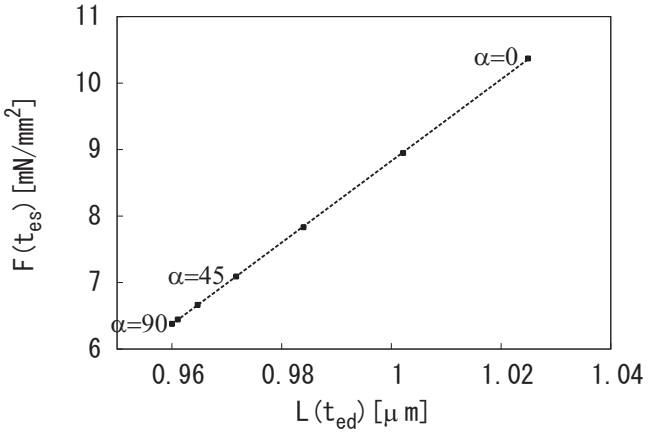

Figure 5: The relationship between $L(t_{ed})$ and $F(t_{es})$

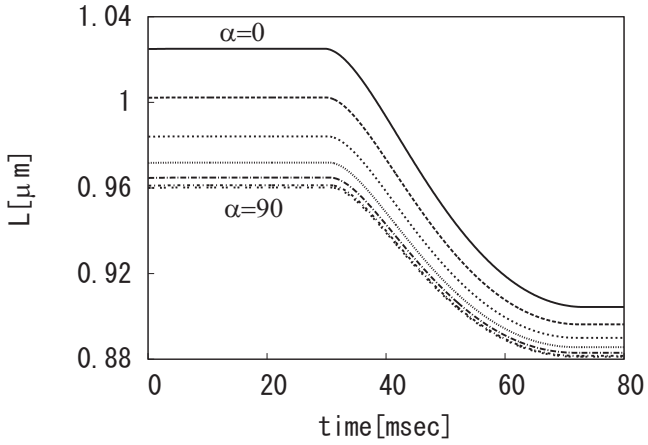

Figure 6: The time course of L

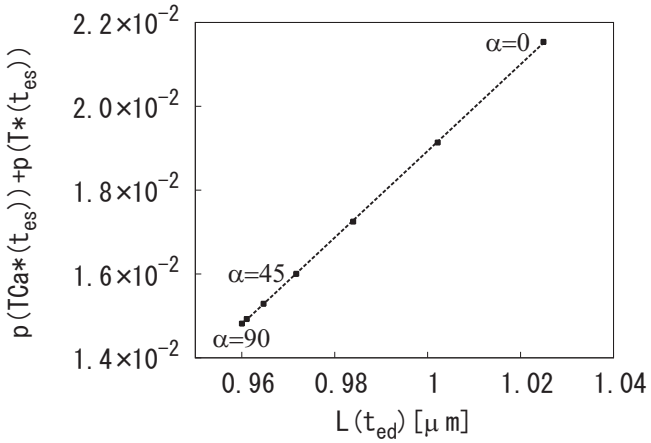

Figure 7: The relationship between $p(TCa*) + p(T*)$ at t_{es} and $L(t_{ed})$

Table 1: The coefficients of determinations of $p(TCa*)$ and $p(T*)$

time[msec]	R^2 of $p(TCa*)$	R^2 of $p(T*)$
10	0.9999	0.9999
20	0.9999	0.9999
30	0.9999	0.9999
40	0.9998	0.9998
50	0.9997	0.9997
60	0.9997	0.9997
70	0.9997	0.9997
t_{es}	0.9997	0.9997

Eq. 24 is much smaller than the linear term in the range of the half sarcomere length (L) in the simulation results (Fig. 6), F_p is approximately linear with L. Therefore, F_b at end-systole ($F_b(t_{es})$) has a linear relation with the half sarcomere length at end-diastole ($L(t_{ed})$). With respect to Eq. 23, the value of $L - X$ at end-systole is close to h_c according to Eq. 10, so $L - X$ can be regarded as constant. Because A and $[T_t]$ are constant, $p(TCa*)+p(T*)$ at t_{es} has an approximately linear relation ($R^2 = 0.999$) with $L(t_{ed})$ as shown in Fig. 7.

In the simulation results, both $p(TCa*)$ and $p(T*)$ have linear relations with $L(t_{ed})$ at any time from 0 to t_{es}. The coefficients of determinations at several points are shown in Table 1. This gives that $\frac{d}{dt}p(TCa*)$ and $\frac{d}{dt}p(T*)$ have also linear relations with $L(t_{ed})$ at any time from 0 to t_{es}. From the model definition described in sec 2.2,

$$\begin{aligned}
&\frac{d}{dt}p(TCa*) + \frac{d}{dt}p(T*) \\
&= Q_2 - Q_4 - Q_5 \\
&= Y_2 \cdot f_{OL}(L) \cdot p(TCa) \\
&\quad - Z_2 \cdot p(TCa*) - Y_4 \cdot p(T*) \\
&\quad - Y_d \cdot f_{CB}(dX/dt) \cdot \{p(TCa*) + p(T*)\}. \qquad (26)
\end{aligned}$$

In this equation, the former three terms are dominant as shown in Fig. 8, 9. Y_2, Z_2 and Y_4 are almost constant as shown in Fig. 10, because $[ATP_{total}]$ and $[PI]$ are almost constant in physiological conditions in Kyoto model. In the simulation result, $p(TCa)$ is nearly independent of α as shown in Fig. 11. As a Taylor expansion of Eq. 8 around a value L_m, $f_{OL}(L)$ can be expressed as

$$\begin{aligned}
&f_{OL}(L) = f_{OL}(L_m) \\
&- 40(L_m - 1.17) \cdot f_{OL}(L_m) \cdot (L - L_m) \\
&+ 40\left\{40(L_m - 1.17)^2 - 1\right\} \cdot f_{OL}(L_m) \cdot (L - L_m)^2 \\
&\qquad + \cdots . \qquad (27)
\end{aligned}$$

In the simulation results, the maximum variation of L with the change of α is 0.9602-1.025 as shown in Fig. 6. In this range of L, the terms of second and more degrees in Eq. 27 can be omitted by setting L_m the median value of the range, so $f_{OL}(L)$ is an approximately linear function of L. Although the time courses of L depend on α, the transition shapes are almost identical, when they are normalized as the maximum to be 1 and the minimum to be 0 as shown in Fig. 12. Thus, L can be approximately expressed as

$$L^{\alpha}(t) = \left\{a_1 L^0(t) + b_1\right\} \cdot L(t_{ed}) + a_2 L^0(t) + b_2, \quad (28)$$

where L^{α} denotes L at α, and a_1, b_1, a_2 and b_2 are constants. Therefore, $f_{OL}(L)$ has an approximately linear relation with $L(t_{ed})$. Consequently, Eq. 26 is approximately linear with $L(t_{ed})$.

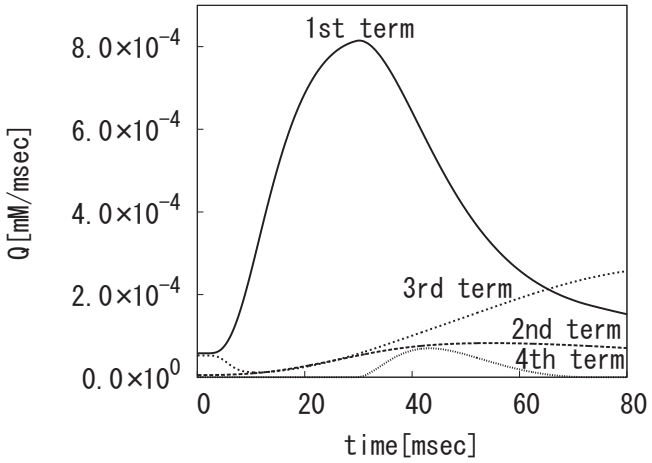

Figure 8: The time course of terms of Eq. 26 at $\alpha = 0°$

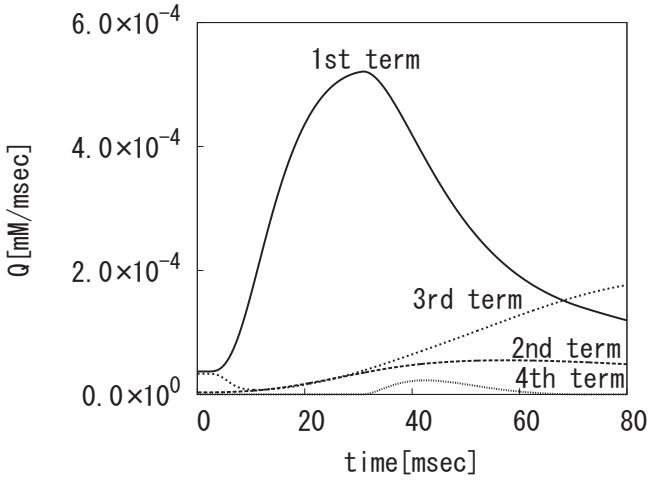

Figure 9: the time course of terms of Eq. 26 at $\alpha = 90°$

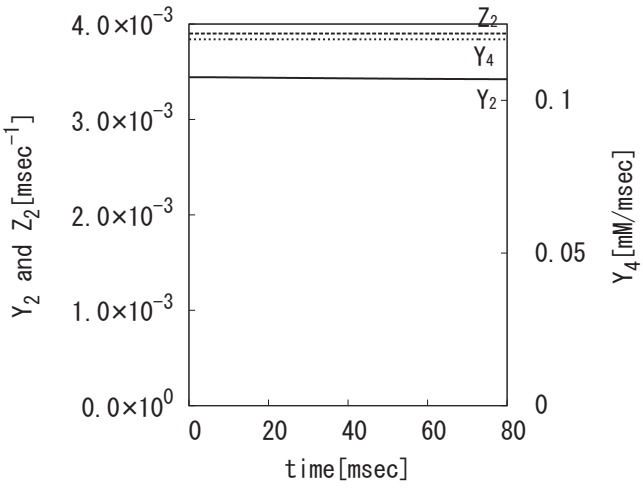

Figure 10: The time course of Y_2, Z_2 and Y_4

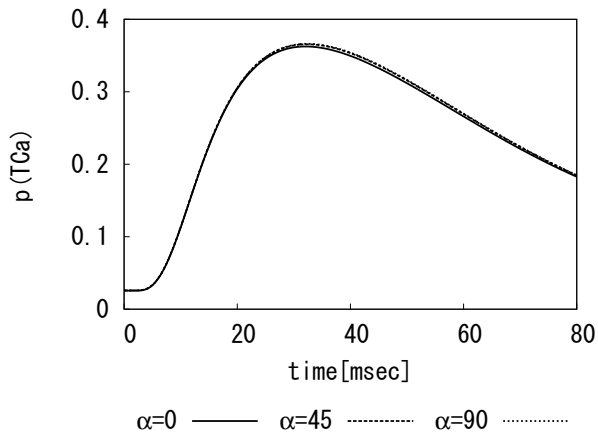

Figure 11: The time course of $p(TCa)$

4 Conclusion

In order to understand the underlying mechanism of Frank-Starling law, we analyzed in depth simulation results of a constructive hemodynamic model, which successfully reproduced a linear ESPVR and a linear relation between end-systolic pressure and end-diastolic volume. The analysis indicates two important factors for the linear relation between end-systolic pressure and end-diastolic volume; 1. microscopical linearity of the force-length relationship of a myocardial cell, 2. independency of the transitional shape of a half sarcomere length from the cardiac load. In the present study, the linear relation was analyzed by decomposing the simulation results. As a future work, we plan a mathematical proof of the linear relation between the developed tension and the half sarcomere length on the excitation-contraction coupling model. In addition, an analysis of the linear ESPVR is also a future work.

References

[1] S. W. Patterson and E. H. Starling. On the mechanical factors which determine the output of the ventricles. *J. Physiol*, 48(5):357–379, 1914.

[2] Toshinori Hongo and Tsutomu Hiroshige. *Hyojunseirigaku 5th edition*. Igakushoin, 2000.

[3] H suga, K Sagawa, and A. A. shoukas. Load independence of the instantaneous pressure-volume ratio of the canine left ventricle and effects of epinephrine and heart rate on the ratio. *Circulation Research*, 32:314–322, 1973.

[4] Hiroyuki Suga, Miyako Takaki, Yoichi Goto, and Kenji Sunagawa. *Shinzourikigaku to enajethikusu*. Koronasha, 2000.

[5] Yutaka Nobuaki, Akira Amano, Takao Shimayoshi, Jianyin Lu, Eun B. Shim, and Tetsuya Matsuda. Infant circulation model based on the electrophysiological cell model. *IEEE EMBS*, 2007.

[6] Thomas Heldt, Eun B. Shim, Roger D. Kamm, and Roger G. Mark. Computational modeling of cardiovascular response to orthostatic stress. *J Appl Physiol*, 92:1239–1254, 2002.

[7] Masanori Kuzumoto, Ayako Takeuchi, Hiroyuki Nakai, Chiaki Oka, Akinori Noma, and Satoshi Matsuoka. Simulation analysis of intracellular Na^+ and Cl^- homeostasis during β1-adrenergic stimulation of cardiac myocyte.

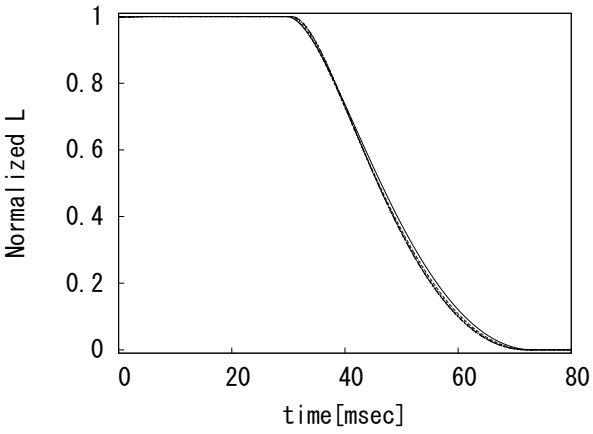

Figure 12: The time course of normalized L

Progress in Biophysics and Molecular Biology, 96:171–186, 2007.

[8] Jorge A. Negroni and Elena C. Lascano. Concentration and elongation of attached cross-bridges as pressure determinants in a ventricular model. *J Mol Cell Cardiol*, 31:1509–1526, 1999.

[9] Sarai N, Matsuoka S, and Noma A. simbio: A java package for the development of detailed cell models. *Biophysics and Molecular Biology*, 90:360–377, 2006.